

## Direct Growth Graphene Via Atmospheric Pressure Chemical Vapour Deposition

Anis Amirah Alim<sup>a</sup>, Roharsyafinaz Roslan<sup>a</sup>, Sharipah Nadzirah<sup>a</sup>, Chang Fu Deea<sup>a</sup>, Muhammad Azmi Abdul Hamid<sup>b</sup> and Azrul Azlan Hamzah<sup>a\*</sup>

<sup>a</sup>Institute of Microengineering and Nanoelectronics, National University of Malaysia, 43600 Bangi, Selangor, Malaysia.

<sup>b</sup>Department of Applied Physics, Faculty of Science and Technology, National University of Malaysia, 43600 Bangi, Selangor, Malaysia.

\*Corresponding author. Tel.: +60 193393429; e-mail: azlanhamzah@ukm.edu.my

### ABSTRACT

The integration of graphene in field-effect transistor (FET) has aroused tremendous attention in the field of sensor technology, particularly for electronic biosensors. However, transferring graphene from metal substrates has destructive effects on the electrical characteristics of the graphene film, leading to severe impurities and defects. Here, we investigated a new approach of technique to synthesis direct-growth semiconducting graphene via atmospheric pressure chemical vapour deposition (APCVD) method. In this study we observe the effects of different reaction times, carbon concentrations and temperatures on the carbon arrangement in graphene. The synthesised graphene was characterised by Raman spectroscopy and field emission scanning electron microscopy (FESEM) to observe the quality of graphene formation. From the Raman analysis, the I2D/IG ratio < 1 indicates the formation of graphene in multiple layers. The ID/IG ratio < 1 was also observed, indicating that the graphene has less disorder of defects. Based on the electrical measurement of the material at estimated distance of 250  $\mu\text{m}$ , a higher I2D/IG ratio leads to a higher resistance. Full width at half maximum (FWHM) of 2D band shows graphene with the highest I2D/IG ratio has the lowest value of FWHM. As the conclusion, these directly grown semiconducting graphene layers can be efficiently integrated into biosensors without any complex post-treatment process.

**Keywords:** Graphene, atmospheric pressure chemical vapour deposition, Raman analysis, FESEM, defects

### 1. INTRODUCTION

Novoselov et al. discovered graphene in 2004, and since then graphene has proven to be the comprehensive inventions of the post-silicon era because of its remarkable and interesting properties: small thickness, huge surface to volume ratio, very small mass and high mobility of charge carriers [1]. These excellent properties of graphene in electrical and optical applications contributed to a far-reaching approach for a scalable and cost-effective method [2]. Graphene, as a stable two-dimensional atomic film with  $\text{sp}^2$  hybridized carbon atoms with unique characteristics, has become the most promising material to be applied in sensors. To date, the method of chemical vapour deposition (CVD) has proven to synthesis high-quality single-layer graphene on a metal substrate [3].

Conventionally, the growth of graphene on metal catalyst can be done using low pressure CVD (LPCVD) [4], [5], plasma-enhanced CVD (PECVD)[6], [7] and atmospheric pressure CVD (APCVD)[8], [9]. However, graphene grown on metal substrates must be transferred to dielectric substrates for electronic applications which known as post-treatment process. There are several processes for transferring graphene including etching transfer, mechanical exfoliation and bubbling transfer. These complex process produces contaminations of polymer film [10], extensive wrinkling [11] and breakage of graphene, which decreases the performance of the final devices.

The residue from the removal of the polymer reinforce layer (i.e. poly methyl meth acrylate (PMMA)) can impair the electrical capabilities of graphene electronics (i.e graphene field effect transistors (FETs)) because they act as boundaries between the scattering centre of carriers and the metal [12]. However, graphene is highly vulnerable to absorbents and molecules that come into contact with its surface, so the PMMA tend to act like a doping agent for the graphene. To achieve ultraclean sample, post-treatment process must be done which increases the complication of the preparation process and the production cost and not suitable for mass production applications [13].

Direct growth graphene on target substrates could be the solution to avoid complex post-processing methods. The growth of graphene using metal-assist is like the common CVD technique, as the carbon source is easily to break up, and the growth rate is accelerated under the similar conditions due to the introduction of a metal catalyst. The most common metals used is copper and nickel. Ismach et al. have demonstrated the direct growth of graphene using the LPCVD method by controlling the dewetting of the copper catalysts after 5 hours of growth. The presence of creases and folds on the graphene leads to midgap states that affect the conductivity of the material [14].

Direct growth of graphene on insulating substrates without metal catalyst was described by Jang et al. using ammonia assisted PECVD [4], but PECVD can cause indemnity impairment to the graphene surface due to

high-energy plasma ions. Moreover, low-pressure and plasma-assisted CVD requires high-priced and specialised instruments, which increases the cost of mass production of the device.

Here we present a facile two-step method to synthesis graphene directly on insulating substrates with metal-assisted by using chemical vapour deposition at atmospheric pressure (APCVD) method. Methane ( $\text{CH}_4$ ) was used as carbon precursor to initiate graphene nucleation. This has been proved by Shan et al. by using copper acetate as metal catalyst to facilitate the direct growth of graphene on sapphire at a temperature of 1020 – 1080 °C by APCVD method [15]. The graphene films obtained showed favourable electrical performance with a sheet resistance of 1.24 k $\Omega$  and a carrier mobility of 8500  $\text{cm}^2 \text{V}^{-1} \text{s}^{-1}$ . Growth time, gas flow rate and temperature are three important factors which will be observed in this study [16].

## 2. THEORETICAL BACKGROUND

The nature of pristine graphene is theoretically hydrophobic which means the surface does not interact with ions and aqueous solutions due to the non-polar nature of the carbon  $sp^2$ [17]. However, several studies show that the presence of defects in graphene (vacancies, dopants or functional groups) could alter the graphene to be hydrophilic. Moreover, the synthesis of pristine graphene is quite complex, and in reality, there are defects in graphene materials that usually originate from different synthesis methods [18].

Our hypothesis in this study is the existence of defects in graphene can increase the sensitivity of the sensors. Lee et al. were able to enhance the sensitivity of chemical sensors by up to 33% when measuring  $\text{NO}_2$  and 614% when measuring  $\text{NH}_3$ [19]. Angizi et al. reported the application of defect-engineered graphene in pH sensors, where the appearance of functional groups on the graphene increased the sensitivity of the sensors[20]. Cho et al. also exhibited the implementation of defect-engineered graphene by directly synthesis graphene mesh structure using silica-assisted chemical vapour deposition method. The study utilise FET for their sensors to study the respond at different pH values[21]. Based on the previous study, we believe vast of room for improving the sensitivity of graphene sensors via defect-engineered graphene and the study in FET-based DNA detection biosensor is still limited.

FET biosensors (BioFETs) essentially consist of source, drain and gate for the electrical electrode and semiconductor material as transducer in the channel region which give electrical responds in chemical or biological interactions. BioFETs have shown excellent characteristics as high sensitivity and high selectivity biosensors with very low volumes of analytes [22]–[24]. In this study, we focused on the effects of different parameters on the synthesis of direct growth defect graphene for the application of biosensors in the future by

observing the quality of graphene and the electrical characteristics.

## 3. METHODOLOGY

All the chemicals applied in this study were purchased from Sigma Aldrich. P-type silicon wafer <100> with boron-doped and silicon oxide thickness of 300 nm obtained from Silicon Materials Inc.

### 3.1 Synthesis of Graphene

The graphene layers were synthesised directly via an atmospheric pressure chemical vapour deposition (APCVD) process. Figure 1 describes all the processes. Preceding to the process, the substrates were cleaned with acetone, ethanol and deionised water in an ultrasonic bath for 10 minutes and subsequently dried at 120 °C on a hot plate. The substrates were then sputtered with a thin layer of Cu using DC magnetron sputtering at 200 V and a pressure of 10mTorr to achieve thickness of 5 nm. This nanolayer Cu was sufficient to act as metal catalyst for graphene growth. This method was referred from previous work where the researchers used Nickel as metal catalyst for graphene growth [25]. The application of copper should allow better control of the number of layers due to the low solubility of carbon [26], [27]. To analyse the effects of various parameters on the formation of graphene, the graphene layers were synthesised in 4 different conditions at varied temperatures, reaction time and flow rate based on Table 1. No post-treatment process was involved.

**Table 1** Different conditions applied for graphene growth

| Conditions / Parameters | Temperature (°C) | Reaction Time (min) | Flow Rate (sccm)  |                 |
|-------------------------|------------------|---------------------|-------------------|-----------------|
|                         |                  |                     | Ar/H <sub>2</sub> | CH <sub>4</sub> |
| A1                      | 900              | 60                  | 100               | 40              |
| A2                      | 900              | 60                  | 100               | 80              |
| A3                      | 1000             | 60                  | 100               | 40              |
| A4                      | 900              | 45                  | 100               | 40              |

Initially the Cu sputtered substrates were placed in a horizontal quartz tube and then purged with Ar/H<sub>2</sub> gas for 30 min to remove any contamination on the substrate and stabilise the system environment. The graphene was growth in a horizontal reactor at temperatures ranging from 900 °C to 1000 °C, at atmospheric pressure. The gas mixture of Ar and H<sub>2</sub> at 97% and 3 %, respectively is fixed at 100 sccm. On the other hand, the flow rate of CH<sub>4</sub> ranged from 40 sccm to 80 sccm.

The growth reaction time occurred when CH<sub>4</sub> was presence at designated temperature, and varied from 45 min to 60 min. Each condition A<sub>2</sub>, A<sub>3</sub> and A<sub>4</sub> were varied for at least one factor by comparing with condition A<sub>1</sub>.

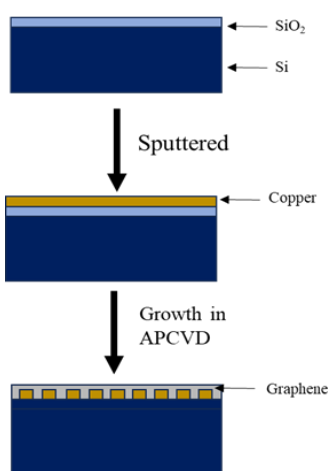


Figure 1. Process of graphene synthesis.

### 3.2 Characterisation

All the samples were characterised by Raman spectroscopy (Thermo Scientific DXR2Xi) analysis. The analysis were performed with a laser excitation wavelength of 532 nm with 900 lines/mm diffraction grating and optical objective of 100x at room temperature. By fitting Lorentzian functions to the data, full widths at half maximum (FWHM) and band intensities were determined. The bandwidth and intensity ratio values for each sample were discovered by Raman maps over  $\sim 50 \mu\text{m} \times 50 \mu\text{m}$  areas on various positions on the sample surface and quantifying the median values over all positions. Raman spectra indicated the ratio between the intensities of the D and G bands,  $I_D/I_G$  ratio which is proportional to the number of structural defects or reduced  $sp^2$  lattice size. The ratio between the 2D band and the G band of the Raman spectra,  $I_{2D}/I_G$  represent the number of layers in graphene [28].

The morphology of the graphene layers was investigated by using field emission scanning electron microscopy (FESEM) (Zeiss Supra 55VP). Using the same machine, energy dispersive X-ray spectroscopy (EDX) element mapping was done to observe the element distribution on the sample. The resistance of the material was determined with a two-point probe system with needles a tan estimated distance of  $250 \mu\text{m}$  using Keithley 2400 Source Meter SMU instruments in DC mode.

## 4. RESULTS AND ANALYSIS

### 4.1 Band Intensities at $\text{CH}_4$ Concentration

The graphene samples were grown at different  $\text{CH}_4$  concentrations based on conditions  $A_1$  and  $A_2$  at atmospheric pressure and growth reaction time of 60 mins at  $900^\circ\text{C}$ . Condition at  $A_2$  has higher concentration of  $\text{CH}_4$  compared to  $A_1$ . The quality of the arranged graphene layers was assessed by Raman spectra. Based on Figure 2, the Raman spectra obtained shown that graphene grown in condition  $A_1$  have higher defects (0.89) and lower layers of graphene (0.16) compared to the graphene grown in  $A_2$

conditions ( $I_D/I_G = 0.45$ ,  $I_{2D}/I_G = 0.53$ ). This shows that higher concentration of  $\text{CH}_4$ , the number of graphene layers increases due to the higher supply of C atoms.

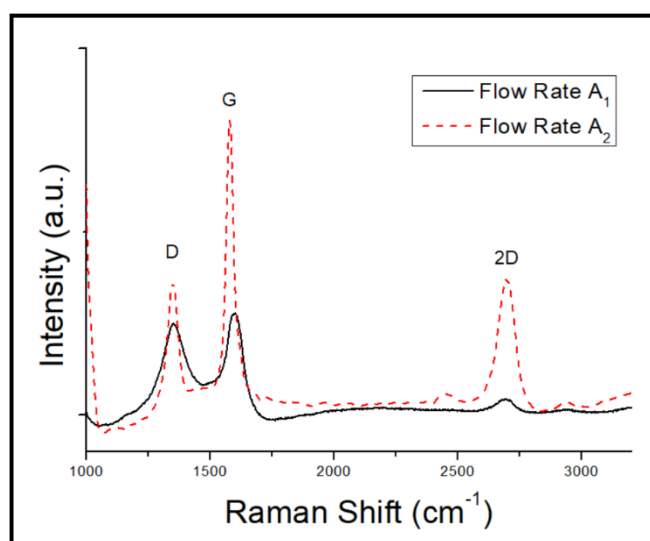


Figure 2. Raman spectra at  $A_1$  and  $A_2$  conditions.

### 4.2 Band Intensities at Varied Temperatures

The direct grown graphene layers were synthesized at different ranging temperatures of  $900^\circ\text{C}$  and  $1000^\circ\text{C}$  at fixed flow rate of gas mixture and growth reaction time was fixed at  $900^\circ\text{C}$ . Based on the Raman spectra shown in Figure 4, the  $I_D/I_G$  ratio increases from 0.89 to 1.56. Higher temperatures during growth contribute to higher defects of the graphene formation. However, there are slightly incremental changes in the  $I_{2D}/I_G$  ratio showing better quality of graphene growth in  $A_3$  condition compared to  $A_1$  condition.

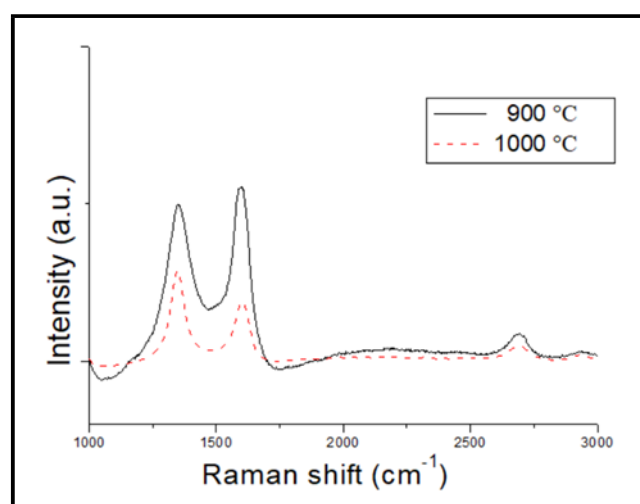
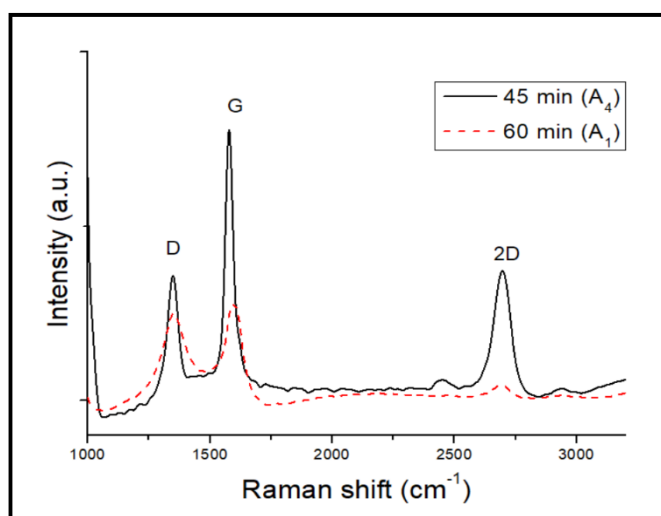


Figure 4. Comparison of Raman spectra at different temperatures.

### 4.3 Band Intensities at Varied Growth Reaction Time

Direct growth graphene by comparing at different growth reaction time shows a significant change based on Figure 5. The graphene layers were synthesised at fixed gas mixture and temperature of 900 °C. The growth reaction time can be defined as the duration time the carbon precursor is supplied into the system. The presence of carbon source initiates the graphene nucleation on the surface of sputtered copper thin film. Increasing of reaction time during growth resulting in mildly reduce graphene oxide, based on the decreasing of 2D band intensity. Longer exposure to high temperatures resulting in decreasing of quality of the graphene ( $I_{2D}/I_G = 0.44$  to  $I_{2D}/I_G = 0.16$ ) and increasing of defects ( $I_D/I_G = 0.43$  to  $I_D/I_G = 0.89$ ).



**Figure 5.** Comparison of Raman spectra at different growth reaction time.

### 4.4. Full Widths at Half Maximum (FWHM)

Table 2 shows the whole results of  $I_{2D}/I_G$  ratio,  $I_D/I_G$  ratio and full width at half maximum (FWHM). The FWHM of 2D band indicates the crystallinity of graphene and numbers of layers in graphene. Narrow or lower FWHM value indicates a high level of crystallinity and low level of  $sp^2$  disorder which have good correlation with the increase of  $I_{2D}/I_G$  ratio [29]. From Table 2, condition A<sub>2</sub> has the lowest value of FWHM which means the graphene formation in condition A<sub>2</sub> is the highest quality of graphene in this study.

**Table 2**  $I_{2D}/I_G$  ratio,  $I_D/I_G$  ratio and full width at half maximum (FWHM) for all conditions

| Condition      | ID/IG Ratio | I2D/IG Ratio | FWHM (cm <sup>-1</sup> ) |
|----------------|-------------|--------------|--------------------------|
| A <sub>1</sub> | 0.89        | 0.16         | 76.09528                 |
| A <sub>2</sub> | 0.45        | 0.53         | 61.24575                 |
| A <sub>3</sub> | 1.56        | 0.29         | 68.06676                 |
| A <sub>4</sub> | 0.43        | 0.44         | 67.96455                 |

### 4.4 Morphology Analysis

Morphology characterisation of graphene layers on substrate reveals various formation of graphene. Figure 6(a) shows the formation of graphene from plane-view which is grown in condition A<sub>1</sub>. The circular shape observed on the substrate indicates the dewetting of the copper catalyst. From the plane-view, graphene was hardly observed compared to the bird's eye view. The small picture in the red box shows the formation of graphene on copper like a 'blanket'. This image is correlated with the EDX element mapping analysis. The presence of copper in graphene does not degrade the graphene application. Moreover, several studies have shown that presence of copper nanoparticles in graphene increase the sensitivity of the sensors [30], [31].

Figure 6(b) shows the results of graphene growth with highest supplied of methane compared to others (condition A<sub>2</sub>). The graphene sheets were crumbling or out of plane on the surface of substrates. The occurrence of defects on graphene can contribute to the increasing of sensitivity in sensors due to the existence of functional groups [19]. Defects in graphene also increase the active sites for biomolecules absorptions [32].

Figure 6(c) demonstrates the structure of carbon nanotubes in the range 111.7 nm to 178.6 nm randomly grown on the surface of the substrate at condition A<sub>3</sub>. We observed that higher temperature during growth time causes the carbon arrangement to roll-up into a tube-like structure.

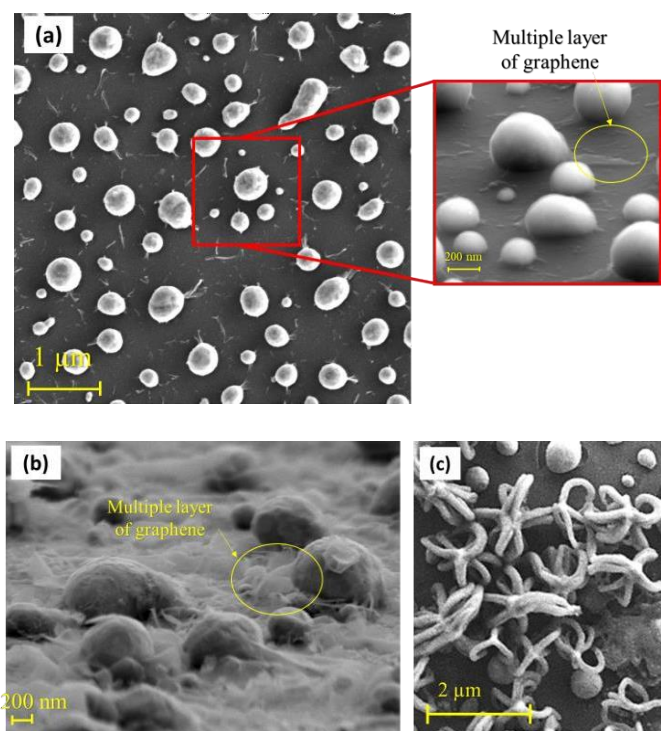


**Figure 6.** FESEM characterisation. (a) Graphene growth at A<sub>1</sub> condition with in-lens detector, smaller picture shows from the bird's eye view (b) Graphene growth at A<sub>2</sub> condition with SE detector at bird's eye view (c) Carbon nanotubes growth at A<sub>3</sub> condition observed at plane-view using SE detector.

#### 4.5 Elemental Mapping Analysis

The formation of graphene on Figure 6(a) is barely observed in the FESEM. We have therefore carried out an element mapping analysis to observe the distribution of the elements C (carbon). We found that element C is evenly distributed on the sample, but the distribution of element O is denser on the surface. This could explain why the Raman spectra of condition A<sub>1</sub> resemble the Raman spectra of reduced graphene oxide. The graphene appears to be multiple layers based on Raman spectra and this correlated with the image from FESEM. The FESEM equipment available could not observe single layer graphene.

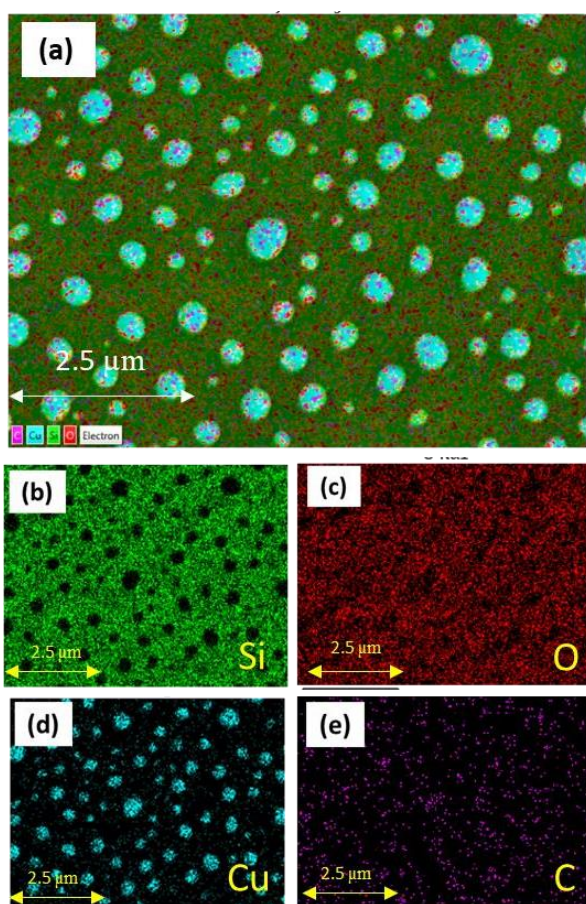


**Figure 7.** EDX mapping analysis for sample growth in condition A<sub>1</sub>. (a) whole sample (b) element Si (c) element O (d) element Cu (e) element C.

#### 4.7 Electrical Measurement

The electrical characteristics of the direct growth graphene on substrate were observed to measure the resistance of the materials. Two-point probe method were used with supplied voltage of max at 5 V at estimated distance of 250 μm.

Figure 8 explains the relationship between  $I_{2D}/I_G$  ratio and the surface resistance of the graphene layers. The  $I_{2D}/I_G$  ratio is proportional to the number of layers of graphene. The higher number of graphene layers increases the carrier mobility which affects the increment in surface resistance [33]. The quality of the graphene formed in

condition A<sub>2</sub> has the highest quality of graphene and the resistance shows a characteristic of a semiconducting graphene [34]. In future work, two electrodes (source and drain) will be deposited on the surface of the graphene with a back-gated electrode. Before fabricating the back-gated FET, the insulating layer for the gate electrode was removed by HF etching [35]. Most BioFETs operated in the range of micro and nano amperes [36]–[38]. The defects observed from FESEM in sample growth at A<sub>2</sub> condition could facilitate the absorption of bioreceptors or biomolecules in biosensors.

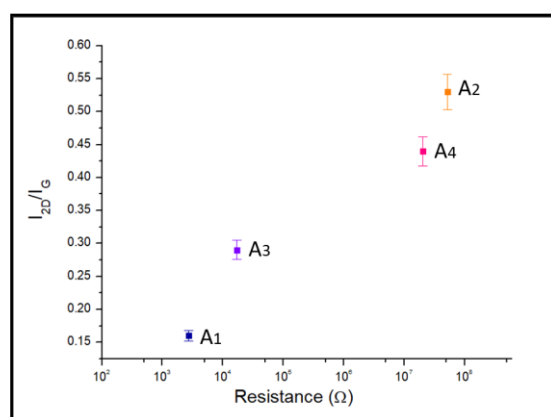


**Figure 8.** The relationship between  $I_{2D}/I_G$  ratio and the surface resistance of graphene.

#### 5. CONCLUSION

In summary, a detailed study on the synthesis of direct growth graphene substrates using atmospheric pressure chemical vapour deposition is presented. We have shown that gas flow rate, temperature and growth reaction time play a fundamental role in the formation of graphene layers. Direct growth graphene at 900 °C with growth reaction time of 60 min and flow rate of Ar/H<sub>2</sub> and CH<sub>4</sub> at 100 sccm and 80 sccm, respectively produce the best quality of defect-engineered graphene. Based on morphology analysis, direct growth graphene can create controllable defects which act as active layers for biosensors application. Further analysis was done to observe the relationship between the quality of graphene and graphene resistance which has the characteristics of semiconducting graphene. The direct deposition of semiconducting graphene for the mass production of electrical devices could become possible through further improvements in the control of the dewetting process.

#### ACKNOWLEDGMENTS

The authors acknowledge the financial support from grant GUP-2019-069. The characterization was done in i-CRIM laboratory, Universiti Kebangsaan Malaysia. The author would also like to thank all the team members for their great assistance and advices.

## REFERENCES

- [1] S. Naghdi, G. Sanchez-Arriaga, and K. Y. Rhee, "Tuning the work function of graphene toward application as anode and cathode," *J. Alloys Compd.*, vol. 805, pp. 1117–1134, 2019, doi: 10.1016/j.jallcom.2019.07.187.
- [2] Z. Li, W. Zhang, and F. Xing, "Graphene Optical Biosensors," *Int. J. Mol. Sci.*, vol. 20, no. 10, p. 2461, May 2019, doi: 10.3390/ijms20102461.
- [3] G. Kalita and M. Tanemura, "Fundamentals of Chemical Vapor Deposited Graphene and Emerging Applications," in *Graphene Materials - Advanced Applications*, 2017. doi: 10.5772/67514.
- [4] J. Jang et al., "Low-temperature-grown continuous graphene films from benzene by chemical vapor deposition at ambient pressure," *Sci. Rep.*, vol. 5, no. 1, p. 17955, Dec. 2015, doi: 10.1038/srep17955.
- [5] A. Jafari, R. Alipour, and M. Ghoranneviss, "The effects of growth time on the quality of graphene synthesized by LPCVD," *Bull. Mater. Sci.*, vol. 38, no. 3, pp. 707–710, 2015, doi: 10.1007/s12034-015-0918-8.
- [6] A. Khalid, M. A. Mohamed, and A. A. Umar, "Graphene growth at low temperatures using RF-plasma enhanced chemical vapour deposition," *Sains Malaysiana*, vol. 46, no. 7, pp. 1111–1117, 2017, doi: 10.17576/jsm-2017-4607-14.
- [7] H. E. Z. Abidin, A. A. Hamzah, M. A. Mohamed, and B. Y. Majlis, "Characterization of Planar Interdigital Micro Supercapacitor with PECVD Graphene as Electrodes at Low Temperature," *Mater. Sci. Forum*, vol. 889, pp. 191–194, Mar. 2017, doi: 10.4028/www.scientific.net/MSF.889.191.
- [8] D. Dutta et al., "Surface topography and hydrogen sensor response of APCVD grown multilayer graphene thin films," *J. Mater. Sci. Mater. Electron.*, vol. 28, no. 1, pp. 157–166, Jan. 2017, doi: 10.1007/s10854-016-5506-1.
- [9] N. Zulkepli, J. Yunas, M. A. Mohamed, M. S. Sirat, and A. A. Hamzah, "Atmospheric Pressure Chemical Vapour Deposition Growth of Graphene for the Synthesis of SiO<sub>2</sub> Based Graphene Ball," *Sains Malaysiana*, vol. 51, no. 6, pp. 1927–1932, Jun. 2022, doi: 10.17576/jsm-2022-5106-27.
- [10] R. S. Selvarajan, R. A. Rahim, B. Y. Majlis, S. C. B. Gopinath, and A. Hamzah, "Ultrasensitive and Highly Selective Graphene-Based Field-Effect Transistor Biosensor for Anti-Diuretic Hormone Detection," *Sensors*, vol. 20, no. 9, p. 2642, May 2020, doi: 10.3390/s20092642.
- [11] V. E. Calado, G. F. Schneider, A. M. M. G. Theulings, C. Dekker, and L. M. K. Vandersypen, "Formation and control of wrinkles in graphene by the wedging transfer method," *Appl. Phys. Lett.*, vol. 101, no. 10, Sep. 2012, doi: 10.1063/1.4751982.
- [12] B. H. Son, H. S. Kim, H. Jeong, J. Y. Park, S. Lee, and Y. H. Ahn, "Electron beam induced removal of PMMA layer used for graphene transfer," *Sci. Rep.*, vol. 7, no. 1, pp. 1–7, 2017, doi: 10.1038/s41598-017-18444-1.
- [13] C. J. An et al., "Ultraclean transfer of CVD-grown graphene and its application to flexible organic photovoltaic cells," *J. Mater. Chem. A*, vol. 2, no. 48, pp. 20474–20480, Oct. 2014, doi: 10.1039/C4TA03432E.
- [14] A. Ismach et al., "Direct Chemical Vapor Deposition of Graphene on Dielectric Surfaces," *Nano Lett.*, vol. 10, no. 5, pp. 1542–1548, May 2010, doi: 10.1021/nl9037714.
- [15] J. Shan et al., "Copper acetate-facilitated transfer-free growth of high-quality graphene for hydrovoltaic generators," *Natl. Sci. Rev.*, vol. 9, no. 7, 2022, doi: 10.1093/nsr/nwab169.
- [16] V. P. Pham, H. S. Jang, D. Whang, and J. Y. Choi, "Direct growth of graphene on rigid and flexible substrates: Progress, applications, and challenges," *Chem. Soc. Rev.*, vol. 46, no. 20, pp. 6276–6300, 2017, doi: 10.1039/c7cs00224f.
- [17] A. Kozbial, F. Zhou, Z. Li, H. Liu, and L. Li, "Are Graphitic Surfaces Hydrophobic?," *Acc. Chem. Res.*, vol. 49, no. 12, pp. 2765–2773, Dec. 2016, doi: 10.1021/acs.accounts.6b00447.
- [18] E. Zaminpayma, M. E. Razavi, and P. Nayebi, "Electronic properties of graphene with single vacancy and Stone-Wales defects," *Appl. Surf. Sci.*, vol. 414, pp. 101–106, 2017, doi: 10.1016/j.apsusc.2017.04.065.
- [19] G. Lee, G. Yang, A. Cho, J. W. Han, and J. Kim, "Defect-engineered graphene chemical sensors with ultrahigh sensitivity," *Phys. Chem. Chem. Phys.*, vol. 18, no. 21, pp. 14198–14204, 2016, doi: 10.1039/c5cp04422g.
- [20] S. Angizi, E. Y. C. Yu, J. Dalmieda, D. Saha, P. R. Selvaganapathy, and P. Kruse, "Defect Engineering of Graphene to Modulate pH Response of Graphene Devices," *Langmuir*, vol. 37, no. 41, pp. 12163–12178, Oct. 2021, doi: 10.1021/acs.langmuir.1c02088.
- [21] S. H. Cho, S. S. Kwon, J. Yi, and W. Il Park, "Chemical and biological sensors based on defect-engineered graphene mesh field-effect transistors," *Nano Converg.*, vol. 3, no. 1, 2016, doi: 10.1186/s40580-016-0075-9.
- [22] R. Song et al., "Detection of MicroRNA Based on Three-Dimensional Graphene Field-Effect Transistor Biosensor," *Nano*, vol. 15, no. 3, pp. 1–8, 2020, doi: 10.1142/S1793292020500393.
- [23] W. Yue, S. Jiang, S. Xu, and C. Bai, "Fabrication of integrated field-effect transistors and detecting system based on CVD grown graphene," *Sensors Actuators, B Chem.*, vol. 195, pp. 467–472, 2014, doi: 10.1016/j.snb.2014.01.071.
- [24] Z. Wang and Y. Jia, "Graphene solution-gated field effect transistor DNA sensor fabricated by liquid exfoliation and double glutaraldehyde cross-linking," *Carbon N. Y.*, vol. 130, no. 7, pp. 758–767, Apr. 2018, doi: 10.1016/j.carbon.2018.01.078.
- [25] H. E. Zainal Abidin, A. A. Hamzah, B. Y. Majlis, J. Yunas, N. Abdul Hamid, and U. Abidin, "Electrical characteristics of double stacked Ppy-PVA supercapacitor for powering biomedical MEMS devices," *Microelectron. Eng.*, vol. 111, pp. 374–378, Nov. 2013, doi: 10.1016/j.mee.2013.03.057.

- [26] A. A. Alim et al., "Carbon nanotubes grown on sputtered copper islands using atmospheric pressure chemical vapor deposition for biosensor applications," in 2023 IEEE 18th International Conference on Nano/Micro Engineered and Molecular Systems (NEMS), IEEE, May 2023, pp. 246–249. doi: 10.1109/NEMS57332.2023.10190858.
- [27] A. A. Hamzah, J. Yunas, B. Y. Majlis, and I. Ahmad, "Sputtered encapsulation as wafer level packaging for isolatable MEMS devices: A technique demonstrated on a capacitive accelerometer," *Sensors*, vol. 8, no. 11, pp. 7438–7452, Nov. 2008, doi: 10.3390/s8117438.
- [28] H. E. Z. Abidin, A. A. Hamzah, and B. Y. Majlis, "Pencirian pertumbuhan lapisan nano grafin di atas elektrod antara digit superkapasitor MEMS," *Sains Malaysiana*, vol. 46, no. 7, pp. 1061–1067, 2017, doi: 10.17576/jsm-2017-4607-07.
- [29] I. V. Komissarov et al., "Micro Raman Investigation of Graphene Synthesized by Atmospheric Pressure CVD on Copper Foil from Decane," *Phys. Procedia*, vol. 72, pp. 450–454, 2015, doi: 10.1016/j.phpro.2015.09.091.
- [30] F. C. Barreto, M. K. L. da Silva, and I. Cesarino, "Copper Nanoparticles and Reduced Graphene Oxide as an Electrode Modifier for the Development of an Electrochemical Sensing Platform for Chloroquine Phosphate Determination," *Nanomaterials*, vol. 13, no. 9, p. 1436, Apr. 2023, doi: 10.3390/nano13091436.
- [31] M. Gupta, H. F. Hawari, P. Kumar, and Z. A. Burhanudin, "Copper Oxide/Functionalized Graphene Hybrid Nanostructures for Room Temperature Gas Sensing Applications," *Crystals*, vol. 12, no. 2, 2022, doi: 10.3390/cryst12020264.
- [32] J. Shao, B. Paulus, and J. C. Tremblay, "Local current analysis on defective zigzag graphene nanoribbons devices for biosensor material applications," *J. Comput. Chem.*, vol. 42, no. 21, pp. 1475–1485, Aug. 2021, doi: 10.1002/jcc.26557.
- [33] B. Galindo et al., "Effect of the number of layers of graphene on the electrical properties of TPU polymers," *IOP Conf. Ser. Mater. Sci. Eng.*, vol. 64, no. 1, 2014, doi: 10.1088/1757-899X/64/1/012008.
- [34] S. Maharubin, X. Zhang, F. Zhu, H. C. Zhang, G. Zhang, and Y. Zhang, "Synthesis and Applications of Semiconducting Graphene," *J. Nanomater.*, vol. 2016, 2016, doi: 10.1155/2016/6375962.
- [35] A. A. Hamzah, B. Y. Majlis, and I. Ahmad, "HF Etching of Sacrificial Spin-on Glass in Straight and Junctioned Microchannels for MEMS Microstructure Release," *J. Electrochem. Soc.*, vol. 154, no. 8, p. D376, May 2007, doi: 10.1149/1.2742302.
- [36] N. N. M. Maidin, R. A. Rahim, M. H. Jacho, N. H. A. Halim, A. S. Z. Abidin, and N. A. Ahmad, "Fabrication of graphene-based back-gated field effect transistor for cortisol detection," *Int. J. Nanoelectron. Mater.*, vol. 11, no. Special Issue BOND21, pp. 123–128, 2018.
- [37] Z. Wang and Y. Jia, "Graphene solution-gated field effect transistor DNA sensor fabricated by liquid exfoliation and double glutaraldehyde cross-linking," *Carbon N. Y.*, vol. 130, no. 7, pp. 758–767, Apr. 2018, doi: 10.1016/j.carbon.2018.01.078.
- [38] D. Sung and J. Koo, "A review of BioFET's basic principles and materials for biomedical applications," *Biomed. Eng. Lett.*, vol. 11, no. 2, pp. 85–96, May 2021, doi: 10.1007/s13534-021-00187-8.